Design optimization and production of a small-scale semi-trailer chassis for testing

Arafat M Ibrahim[1*] , Ahmed M Ali[1] and Hisham Kamel[1]

*Correspondence:
engarafat222@gmail.com

[1] Automotive Engineering Department, Military Technical College, Cairo, Egypt

Abstract

The automotive industry is placing a high priority on the design and optimization of articulated vehicles to minimize the risk of potential accidents or failures. Before mass production, field testing is a crucial step in the development process, requiring extensive dynamic tests to provide a secure design. However, these tests can be both expensive and time-consuming. This study presents the design process of a small-scale low-bed semi-trailer chassis, manufactured to simulate the structural response of an actual semi-trailer. The aim was to identify weak points through analysis under bending conditions and then optimize the thickness and width of the various cross-sections to increase strength while minimizing costs. After manufacturing and welding based on the optimized design, the equivalent chassis was subjected to two load cases for experimental testing. The test results confirmed the accuracy of the finite element analysis, with a deviation of 7.75 to 10.24% in stress levels compared to the numerical results. Overall, this study demonstrates an effective approach to optimize the design of low-bed semi-trailers for improved safety and cost-effectiveness.

Keywords: Finite element, Design optimization, Semi-trailer, Chassis prototyping, Experimental testing, Vehicle structure

Introduction

Vehicle prototype testing, particularly of semi-trailers, is a crucial step in the development process. Following the design phase, thorough testing is imperative to ensure the vehicle's performance, durability, and road safety. According to a study published by the World Health Organization (WHO), the number of worldwide deaths due to road accidents was between 1.25 and 1.35 million per year in 2018, of which heavy vehicles had a main contribution of such accidents [1]. Several researches were conducted to study the safety and stability of heavy vehicles while other were established to investigate the relationship between the drivers' behavior and roadway crashes [2–6]. It was concluded that the contribution between drivers' behavior and vehicle's weight, length, and speed attributed to higher probabilities of road accidents. To guarantee the proper design for a safe vehicles, various methodologies have been developed for testing individual components and parts, including vibration analysis, fatigue analysis, and noise analysis. Currently, both small and large structures are tested to determine vehicle's life under operational loads.

Ibrahim *et al. Journal of Engineering and Applied Science*   (2023) 70:35

Page 2 of 18

The latest computational methods provide a highly efficient way to design heavy vehicles through finite element analysis (FEA). The FEA simulates vehicle structures in different loading scenarios. This helps the designer to efficiently study different design variations in order to find the design that is both lightweight and sufficiently reliable during the expected service life of the vehicle [7, 8]. However, design objectives such as weight and reliability are typically conflicting in nature; therefore, structural design optimization is required to find a feasible design that satisfies all objectives [9–11]. In general, design optimization achieves a balanced trade-off between one or more objectives simultaneously under given circumstances by searching the design space [12–15]. However, it is important to validate the optimum design from FEA with experimental verification tests using real-life simulations, as underestimating applied loads on the chassis can result in catastrophic failures.

Road tests, which involve testing tractors and semi-trailers over an extended period of time to estimate their fatigue life, are frequently performed. However, these tests can be time-consuming and costly, taking several months and requiring especially skilled drivers, as well as incurring expenses for maintenance, fuel, and possible repairs. As a result, most newly designed semi-trailers undergo only rigidity and resistance tests, which are sufficient to validate the design based on numerical analysis.

Malon et al. [16] conducted an analysis and optimization study of a three-axle semi-trailer developed by Zaragoza University. A special-purpose fatigue test bench was developed specifically for this purpose. The test bench was capable of providing maximum torsion to the vehicle without sliding, with the shortest possible cycle duration, which was limited by the hydraulic actuators' maximum displacements and speeds. The optimization process resulted in an innovative fatigue testing profile for semi-trailers, leading to a remarkable reduction in testing duration from years to just 3 months and a significant decrease in total testing costs compared to traditional circuit testing techniques.

Baadkar et al. [17] performed a failure analysis on a self-loading container carrier semi-trailer. The semi-trailer was first modeled using CAD software and subjected to a static FEA to determine potential crack locations during various service conditions. The model was then validated through experimental measurements using strain gauges and geometrical validation using ANSYS element shape-checking. A fatigue analysis was also conducted to determine the possibility of failure in low-strength areas under a selected loading condition. The findings led to the development of a new improved design to prevent future failures at the identified crack locations.

Napierala et al. [18] presented a verification process for a new lightweight semi-trailer structure design featuring bent sheet metal profiles as transverse beams in the curtain frame. A CAD model was developed to study the stress analysis under applied loads. A prototype of the semi-trailer was then manufactured and tested, with two vertical displacement sensors placed directly under the vertical applied load and six strain gauges equipped on the middle crossbar. The experiment produced results that were consistent with the numerical analysis, with similar levels of stress and deflection.

Deulgaonkar et al. [19] provided an analytical and numerical analysis for an off-road chassis-mounted platform. The loading pattern, the platform configurations, and the mounting locations were studied at first. The shear force, section modulus, and bending

moment for each structural member were estimated based on the loading conditions. Also, FEA was carried out for static, gradient, braking, and vertical acceleration cases using shell elements under the same loading and boundary conditions. Then, a scaled prototype with dimensions of 1500 × 1000 mm. was manufactured for establishing experimental tests in the laboratory. That prototype satisfied all the design requirements and configurations of the full-scale platform. Also, it has the same design, positions, orientations, constraints, and dimensions of the several cross-members as the full-scale platform. Finally, static and gradient analyses of the platform were conducted for both the full-scale and the reduced-scale prototype. Experimental measurements for the high-stress areas were established for design verification. A close correlation of stresses between the experimental and the FE results were achieved for static and gradient loading conditions. The strain values in the chassis rear portion were lower than those in the front and the mid portions despite the rear overhung. Consequently, an efficient load transfer from the rear portion to the front and the mid portions was achieved. That load transfer improved the stability of the vehicle on curvy roads.

Akhtar et al. [20] developed a new strategy for improving the FE modeling of bonded flooring structures. These structural improvements were attained by studying the effect of performing shape optimization, using various structural profiles, materials, and plywood panels. Scaled-down models with the different structural profiles of the original semi-trailer were manufactured for experimental testing. These tests aimed to study the effect of altering the design, the used material, and the cross-section shape on the chassis weight and strength. The different zones of the semi-trailer were tested for floor strength and stiffness by studying the scaled-down models using ISO 1496-1 (1990). Then, several experiments were performed to validate the simulations of the UPM Plywood. Also, a comparative study was established based on the experiment and FE results to estimate the critical parameters of the model. The new design provided a weight reduction of 5.28% while changing the shape of the cross-members besides the weight reduction contribution of the longitudinal beams. During the forklift wheel load test, a weight reduction of 3.82% and a 2.88% increment of the model stiffness were achieved for the preliminary design of the flooring structure. On the other hand, a reduction of 9.47% in the deformation of the original semi-trailer with plywood compared to the chassis-only model without plywood during the freight load case.

There are many solutions for transporting goods, but road transportation is regarded as the backbone facility of commerce and transportation all over the world. Complying with the height and length restrictions, versatility, and adaptability are the main reasons behind the massive spread of semi-trailers for heavy cargo transportation. However, the design of heavy vehicles for transportation especially by semi-trailers faces great challenges with safety and stability concerns. Lightweight, durable, and reliable semi-trailers with minimal costs have the main elements of success in competitive markets. Recently, an intensive demand for testing the safety and durability of semi-trailers due to the rapid increase in accidents related to heavy vehicles.

Ibrahim *et al. Journal of Engineering and Applied Science*   (2023) 70:35

Page 4 of 18

Methods and materials

The authors of this study aimed to conduct the design optimization for a small-scale chassis of a low-bed semi-trailer. The original semi-trailer was designed based on fully loaded pure bending conditions [21]. A small-scale equivalent chassis was developed to simulate the structural response of the original semi-trailer and validate the results of the FEA. It was modeled using SOLIDWORKS 2020, while the static FEA was performed using ANSYS Workbench 2020.

A two-dimensional beam element was utilized for modelling the chassis under the applied loads. Also, all joining methods and connections between the chassis beams were considered as welded as the original chassis of the semi-trailer. That idealization and simplification of the chassis case study were established to reduce the computational time and cost without occurrence of numerical errors while still accurately simulating the response of the original chassis.

The base material of the equivalent chassis was structural steel St. 37-2, while the base material of the original chassis is structural steel St. 52-3. The structural steel St. 37-2 is a commercial material with good machinability and weldability. It is commonly used for structural applications as it is widely available in the market in large quantities. It has a high strength-to-weight ratio with a yield strength of an untreated St. 37-2 sheets up to 235 MPa. [22]. But conducting structural steel St. 52-3 as a base material of the equivalent chassis may cause a noticeable increment in the total expenses despite its higher yield strength. Also, structural steel St. 52-3 and St. 37-2 approximately have the same Poisson's ratio, modulus of elasticity, and elongation to break. Thus, the structural steel St. 37-2 can be utilized for manufacturing the equivalent chassis of the semi-trailer.

The dimensions and thicknesses of the main longitudinal members and cross-members were optimized to reduce production costs and manufacture a lightweight yet strong chassis. The optimized chassis was manufactured and assembled, and static experimental measurements were conducted to validate the FE results then the results and observations were discussed. The equivalent chassis design life flowchart is illustrated in Fig. 1.

Design of the equivalent chassis

Semi-trailers are designed to transport heavy cargos over long distances and have the capability to navigate rough terrain and off-road conditions. Their robust and durable design is achieved through advanced computational methods and tools, which provide accurate predictions of the chassis response under both static and dynamic loads. An equivalent structure was manufactured and tested under predefined loads to validate these predictions.

The equivalent chassis is designed to mimic the geometry of the original semi-trailer chassis. The main dimensions of the equivalent chassis are similar to those of the original chassis, with an overall length and width that have been scaled by a factor of 1:6 as illustrated in Fig. 2.

Many attempts were conducted to evaluate the appropriate scaling factor of the equivalent chassis based on the trial and error method. On the one hand, a small-sized chassis may cause many problems in the assembling and welding process due to the small
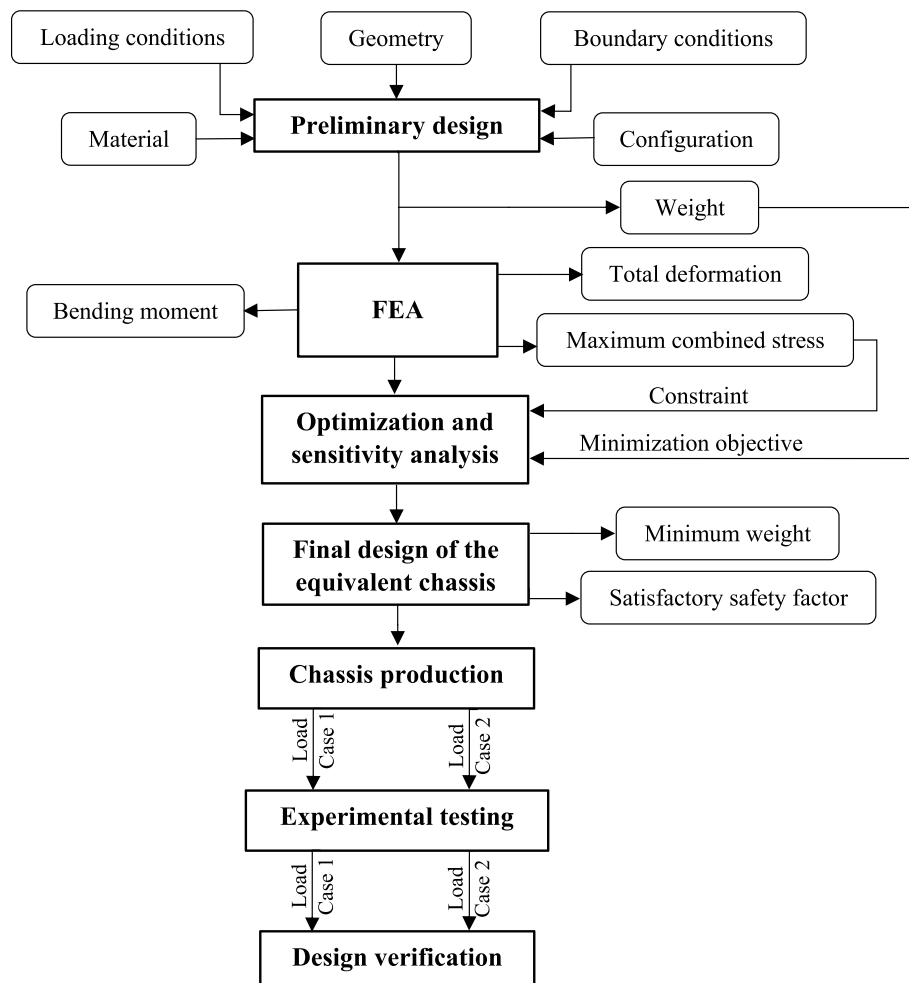
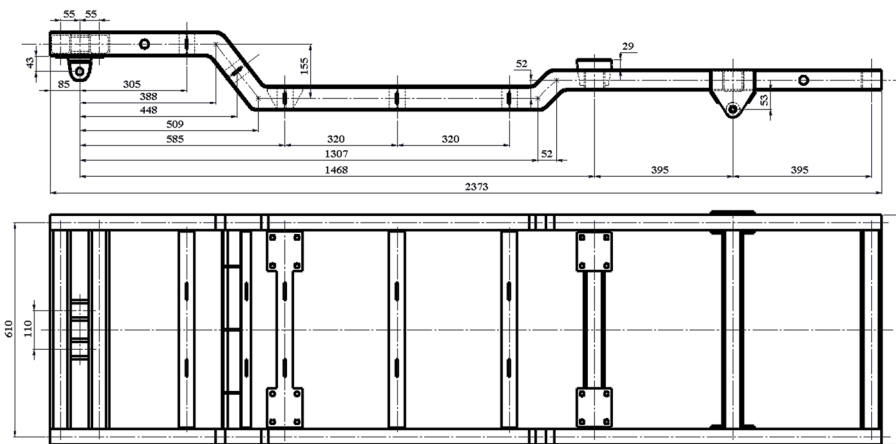**Fig. 1** The flowchart of the equivalent chassis design life cycle

Fig. 2 The main dimensions of the equivalent chassis in [mm]

Ibrahim *et al. Journal of Engineering and Applied Science*   (2023) 70:35

Page 6 of 18

thicknesses of the used material sheets. On the other hand, a full-scaled equivalent structure is costly, heavy needs bulky payloads for testing, and requires special equipment for assembling and welding due to the large thicknesses of the utilized material sheets. That utilized scaling factor 1:6 guarantees the production of lightweight chassis with minimal costs using the available materials and sheet thicknesses.

The equivalent chassis has the same configuration as the original low-bed semi-trailer, including similar cross-section shapes I-beam and box section for the main longitudinal beams and cross members, respectively. The configuration of the equivalent chassis is illustrated in Figs. 3 and 4, and Table 2.

FEA of the equivalent chassis

The equivalent chassis of the semi-trailer was subjected to a single payload of 600 kg, which was divided between the front and rear supports. The front load was considered 1.5 times the rear load, the front support was loaded with 360 kg, and the rear support was loaded with 240 kg. The equivalent chassis was also subjected to the same fixation conditions as the original chassis, with a hinged front kingpin support and roller supports at the rear as illustrated in Fig. 5. The total weight of the equivalent chassis is 77.93 kg based on the selected material and the geometry of the initial design. The distributed loads acting on the supporting beams of the equivalent chassis can be calculated as follows:

$$W_C = \frac{360*9.81}{610} = 5.7895 \ N./mm \ \ W_D = \frac{240*9.81}{610} = 3.8597 \ N./mm$$

Generally, the selection of the appropriate element size for a FE simulation has a direct effect on the solution's accuracy, computational time, and costs. The fine-meshed analysis provides a high-accuracy solution, but the main drawbacks of fine meshing are that it is time-consuming for analysis and added expenses due to the computational costs. Exceeding the number of elements more than specific values considerably consumes extra computational costs and time without affecting the solution accuracy.

While conducting the two-dimensional beam element was for simulating the equivalent chassis, the meshing size has not a noticeable response on the simulation results
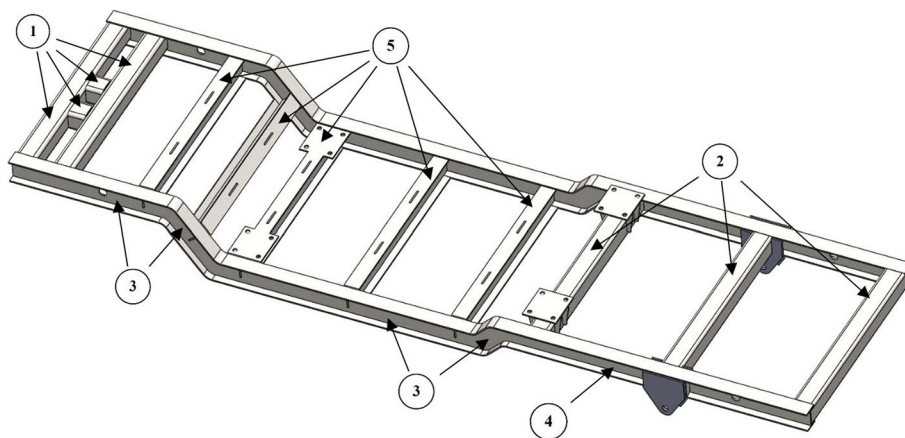
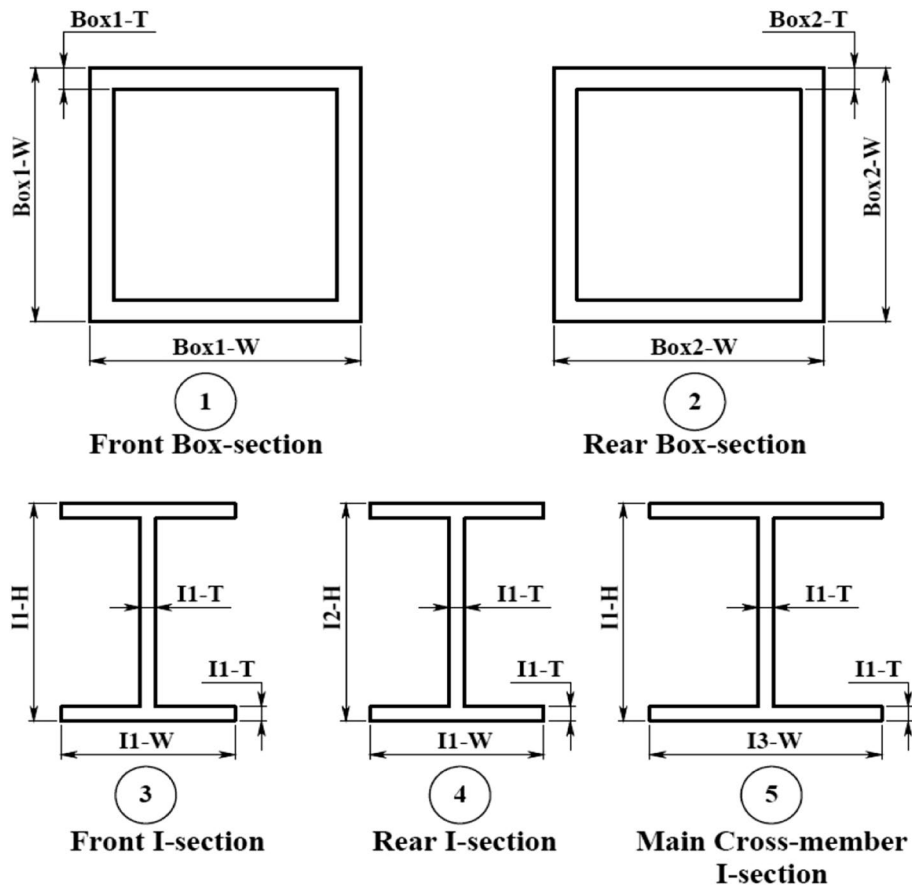**Fig. 3** Three-dimensional modelling of the equivalent structure considering the different cross-sections

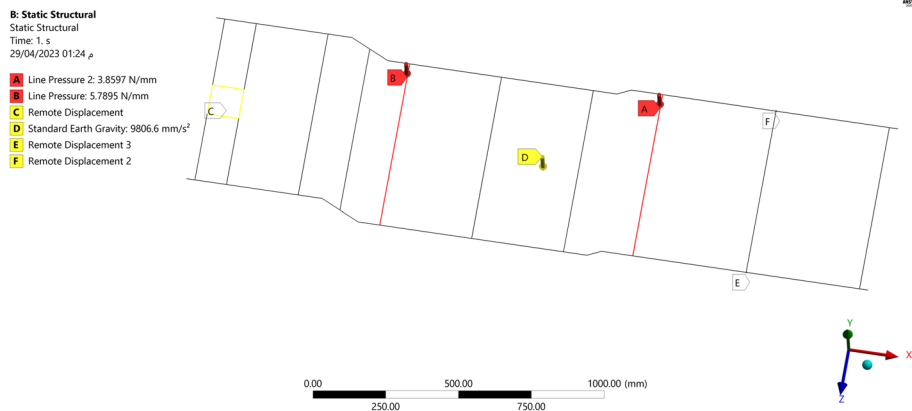**Fig. 4** The various cross-sections of the equivalent chassis (in accordance with Fig. 3)

Fig. 5 The loads and boundary conditions acting on the equivalent structure

Table 1 A comparison between the FE results of the chassis using different element sizes

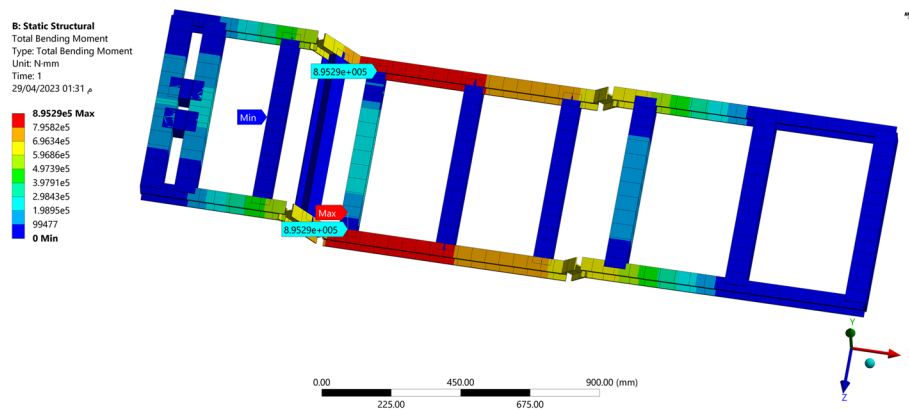|	50 mm element size	0.5 mm element size
Number of nodes	534 node	45066 node
Number of elements	258 element	22524 element
Computational time	11 s	6.5 min.
Maximum combined stress	81.492 Mpa	81.824 Mpa

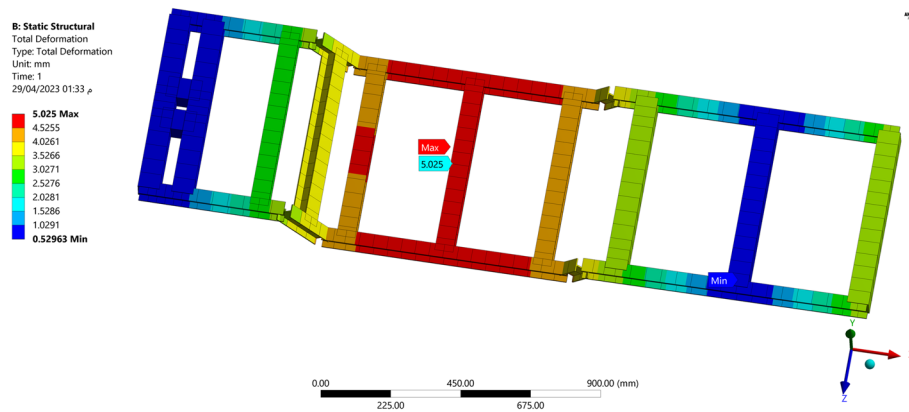**Fig. 6** The total bending moment of the equivalent structure

Fig. 7 The total deformation of the equivalent structure

as illustrated in Table 1. The maximum combined stress that was generated on the chassis was 81.492 Mpa when conducting an element size of 50 mm with a simulation duration of 11 s. While it was 81.824 Mpa, acting on the exact location for a simulation duration of 6.5 min when using a 0.5 mm element size that was 100 times smaller than the original element size. The error between the maximum combined stresses of these two simulation cases was about 0.4%. While the usage of 50 mm element size was about 35.2 times computationally faster for simulating the chassis than the usage of 0.5 mm element size while using seventh generation laptop. Thus, a 50-mm element size was conducted for simulation and optimization of the equivalent chassis to reduce the computational time and the total costs.

Due to the vertical loading conditions, the chassis deformation can be described as a deflection of the chassis structure. The structural responses due to the loading conditions are illustrated as shown in Figs. 6, 7, and 8. The FE results showed that the maximum bending moment on the chassis is 8.9529×10^5 N.mm located in the main longitudinal beam at the place of its connection with the front loading support. Thus, a maximum combined stress of 81.492 MPa was generated at the same position. While the maximum deformation of the chassis is 5.025 mm which occurred in the middle of the chassis exactly at the connection between the middle cross-member and the main longitudinal beam. These findings provide valuable information about
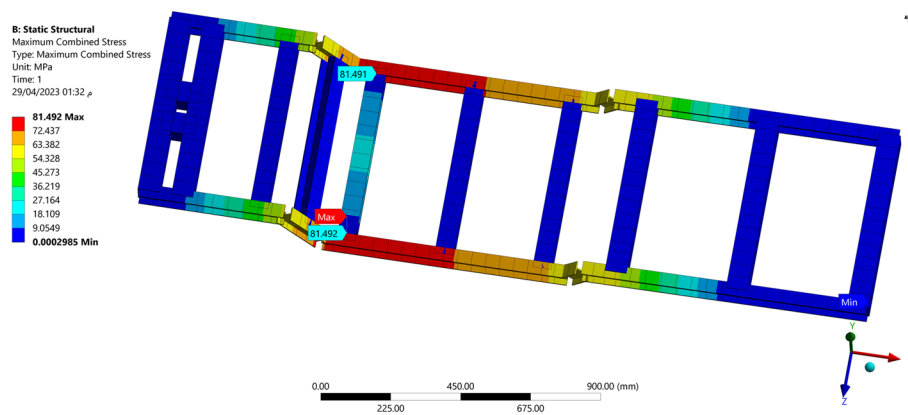
Ibrahim *et al. Journal of Engineering and Applied Science* (2023) 70:35

Page 9 of 18

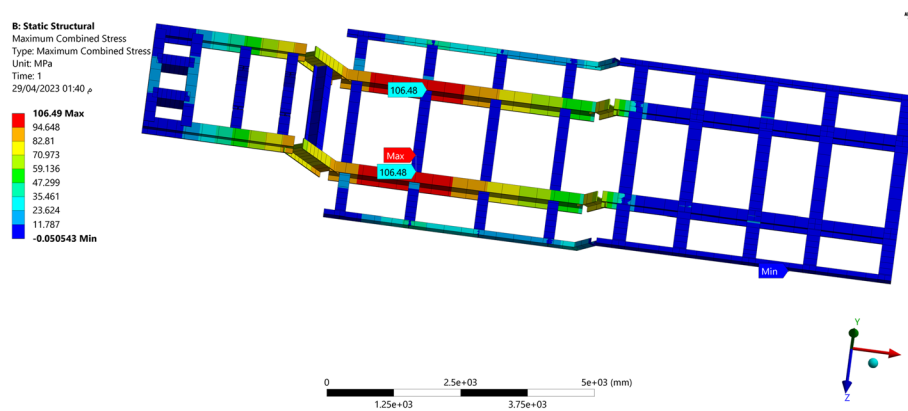**Fig. 8** The maximum combined stresses of the equivalent structure

Fig. 9 The maximum combined stresses of the original chassis

the structural performance of the equivalent chassis and can be used to evaluate its suitability for carrying heavy payloads.

For the original chassis of the semi-trailer, the maximum combined stress is 106.5 MPa due to the vertical loading conditions as illustrated in Fig. 9 [21]. This similarity of the stress patterns between the equivalent and original semi-trailers demonstrates that the equivalent semi-trailer accurately represents the stress and deformation behaviors of the original semi-trailer. It provides a reliable tool for evaluating and analyzing the structural performance of the original semi-trailer under various loading conditions before starting the manufacturing process of the original chassis. This approach considerably reduces computational time and cost. Additionally, it offers a faster evaluation of the original semi-trailer response under various loading conditions, thereby enhancing the efficiency of the design process.

Structural optimization and sensitivity of the equivalent chassis

Optimization of the equivalent chassis

The design optimization of the equivalent chassis is a crucial step before the manufacturing process to minimize the total chassis weight while ensuring that the generated stresses remain within safe levels. Due to the budget constraints of the chassis

Ibrahim *et al. Journal of Engineering and Applied Science*   (2023) 70:35

Page 10 of 18

prototype, two different optimization techniques were equipped to achieve the solution of the optimization problem: Adaptive Single-Objective Optimization (ASO) and Response Surface Optimization (RSO) [23]. Because of the non-linearity of the optimization problem and the diversity and size of the search space, it is difficult to ensure deterministic optimality of the solution method. We considered two different well-known optimization methods to double check and ensure the optimality of yielded solution. The optimal solution of each method may not be identical due to the main differences in the concepts of each algorithm. If there is a convergence between the two solutions of each optimization method, high reliability of the optimization objective can be accomplished.

ASO is an efficient optimization method that was conducted to achieve the optimal design of the equivalent structure by exploring the design space using a minimal number of design points. The failed design points can be considered as inequality constraints that make it fault-tolerant. It is a direct optimization method that conducts the automatic intelligent refinement by assessing the sensitivities and responses of each design parameter using thickness and size optimization to achieve the global optimal solution of the optimization problem [24]. Besides, it is an adaptive gradient-based algorithm that evaluates the best solution by using a combination of the mixed-integer sequential quadratic programming, the optimal space-filling, the design of experiments, and the kriging response surface. Moreover, it can efficiently work with both continuous and manufacturable design variables.

On the other hand, the response surface optimization by ANSYS Workbench can be conducted to accomplish the optimization objective using different mathematical algorithms to fit experimental design points. Various response surface methods can be equipped for solving the optimization problem, such as kriging response surface, standard second-order response surface, non-parametric regression response surface, etc. It was established using a genetic aggregation which conducts a genetic algorithm for solving the different types of the generated response surfaces in parallel. Thus, the genetic aggregation model is more reliable than the classical response surface model as it considers both the accuracy and stability of the response surface at the design point [25].

The optimization problem was formulated based on nine design variables to find five candidate design points that meet the optimization objective. The optimization objective aimed to minimize the total weight of the equivalent chassis while limiting the maximum combined stress up to 67.14 MPa for achieving about 3.5 safety factor. The optimization results of each optimization method showed that the same candidate point was obtained by both methods. Also, it was noticed that the direct optimization method employed more design points and took longer time than the response surface method. The general form for the optimization problem can be described as follows:

$$\text{Minimize}: f(\mathbf{x}) = M = \sum_{e=1}^{n} \rho_e \, A_e(\mathbf{x}) \, L_e(\mathbf{x})$$
$$\text{Subject to}: g(\mathbf{x}) \leq 67.14 \text{ MPa}.$$
$$\text{and}: \mathbf{x}_l \leq \mathbf{x} \leq \mathbf{x}_u$$

The function $f(\mathbf{x})$ describes the total weight function of the semi-trailer, and $g(\mathbf{x})$ is the maximum combined stress σ_e^B inequality constraint. That stress was subjected

Table 2 The initial, final, and upper to the lower limits of the design parameters

	Parameter name	Upper to lower limit	Step	Initial	Final
1	$I1_W$ (mm.)	45:60	5	45	45
2	$I1_H$ (mm.)	60:80	10	60	70
3	$I1_T$ (mm.)	4:6	1	4	4
4	$I2_H$ (mm.)	60:80	10	60	60
5	$I3_W$ (mm.)	45:60	5	60	45
6	$Box1_W$ (mm.)	60:70	5	70	60
7	$Box1_T$ (mm.)	5:6	1	6	5
8	$Box2_W$ (mm.)	60:70	5	70	60
9	$Box2_T$ (mm.)	5:6	1	6	5

to the eth beam element for bending, and **x** is the design variables vector. The design space of the optimization parameters was described by a side constraint with $\mathbf{x}_u$ and $\mathbf{x}_l$ as mentioned in Table 2. The vector containing the design variables is as follows:

$$\mathbf{x} = [I1_W\ I1_H\ I1_T\ I2_H\ I3_W\ Box1_W\ Box1_T\ Box2_W\ Box2_T]^T$$

The ANSYS results after performing optimization for the equivalent chassis are described below:

- The total chassis weight $= 65.789$ kg.
- The maximum deformation of the chassis $= 3.68$ mm.
- The maximum bending moment of the chassis $= 8.9364 \times 10^5$ N.mm.
- The maximum combined stress of the chassis $= 66.27$ MPa.

The optimization solution successfully achieved a 15.6% elimination of the total chassis mass. Also, a 26.75% reduction of the maximum deformation and an 18.7% reduction of the maximum combined stress were accomplished.

Sensitivity of the equivalent chassis

The sensitivity analysis is usually performed to estimate the objectives change due to the variables change during an optimization problem. For a large number of design parameters, sensitivity analysis aims to figure out the most effective parameters of the design to reduce the computational cost and time of the optimization process. Usually, the sensitivity analysis can be evaluated after building the response surface of an optimization problem. It is a built-in tool in ANSYS Workbench that is accompanied by the optimization solution of the FE solution. In this study, local sensitivity was acquired to achieve the norm of the partial derivatives for the adopted objective concerning the selected parameters.

Generally, sensitivity analysis can be defined as the derivative of a performance measure concerning the design parameters [26]. Currently, there are four main methodologies for obtaining the derivatives of structural performance for specific parameters: discrete derivatives, computational or automatic differentiation, overall finite differences, and continuum derivatives. The small differences between those methods directly affect the

shape and meshing sensitivities due to the discretization process of numerical analysis. For a "black box" software, without the availability of accessing the source code, implementation of the discrete or continuum derivatives mainly depends on the possibility of adding user-defined subroutines and accessing the program's database.

The global finite differences method is the most commonly used method for obtaining derivatives due to its simplicity in implementing the sensitivities. It can be equipped entirely without access to the source code. While several software programs estimate the structural sensitivity using the discrete method which was implemented with the semi-analytical approximation as it requires very little programming effort and almost no element-dependent sensitivity routines. The main advantage of the analytical discrete derivatives is that it introduces no approximations, but the associated implementation efforts are tremendous.

In this study, the sensitivity analysis of the equivalent chassis aims to determine the output responses of the design with respect to changes of the various design parameters such as the thicknesses and widths of the chassis beams as illustrated in Fig. 10. The factors affecting the structural mass are flange thickness, width, and front cross-section height, while the factors affecting stress due to vertical loading conditions are flange thickness, front cross-section height, and flange width. The factors affecting structural deformation are front cross-section height, flange thickness, and width.

Production of the equivalent structure

The production of a vehicle chassis, including the equivalent low-bed semi-trailer, is a complex process that involves several manufacturing steps. The equivalent chassis consists of two main longitudinal beams and several cross-member subassemblies. Each subassembly was manufactured and assembled separately using a welding process, as shown in Fig. 11.

The longitudinal beams were produced using a laser-cutting machine, then assembled using clamps and checked for flatness using a fixture before being welded. The I-shape cross-members were cut to size with a laser-cutting machine, assembled, and welded. The box-shaped cross-members were manufactured by cutting rectangular tubes to size
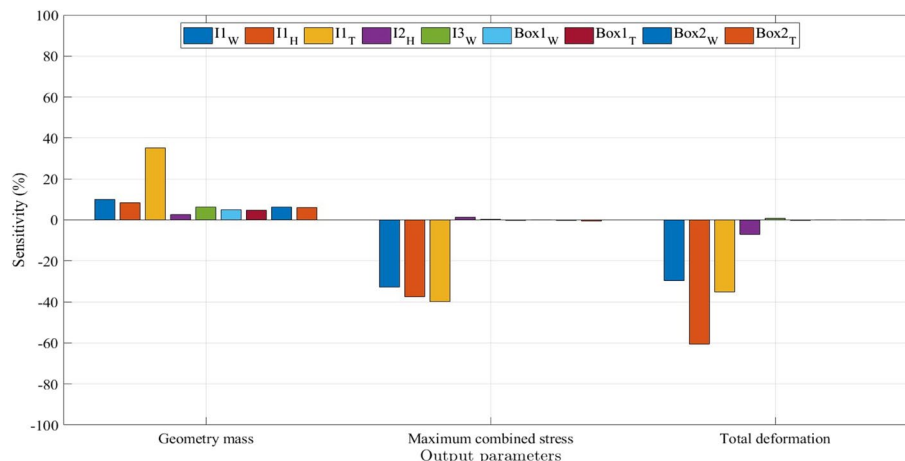

Fig. 10 Sensitivity analysis of the equivalent chassis

Fig. 11 Assembling the main longitudinal beam by a fixture for welding

Fig. 12 The welding process of the I-shape cross-members with the chassis

with a saw-cutting machine and machined with a milling machine before assembly. The chassis frame was assembled using the guiding edges technique, which assures the correct cross-member spacing. Finally, the entire chassis was welded using Metal Inert Gas welding (MIG welding) with a fixture, as shown in Fig. 12. The structure of the equivalent chassis after the manufacturing process is illustrated in Fig. 13.

Static testing of the equivalent chassis

The equivalent chassis was tested under two static load cases to verify the numerical results. Each experimental setup was replicated three times an hour apart between each experiment to check the reliability of the strain gauge results. For the first load case, normal loads of 215 kg and 145 kg were uniformly distributed on the front and rear supports respectively. For the second load case, normal loads of 130 kg and 85 kg were uniformly distributed on the front and rear supports, respectively. The chassis weight was disregarded during the simulation as it had been calibrated during the leveling process.

As the experimental measurements were established for a pure bending static condition of the semi-trailer, the average values of the strain gauge readings can be assessed for verification of the FEA. Thus, four strain gauges were used to measure the generated strain on the chassis due to the loading conditions. Two of these strain gauges were placed under each support of the chassis as depicted in Fig. 14. The strain gauge readings

Fig. 13 The structure of the equivalent chassis after assembling, welding, and painting processes
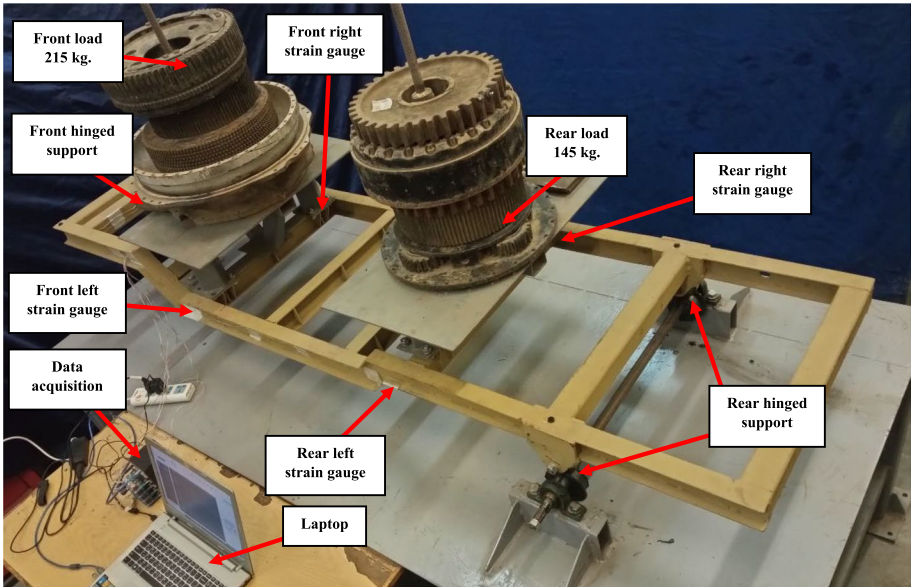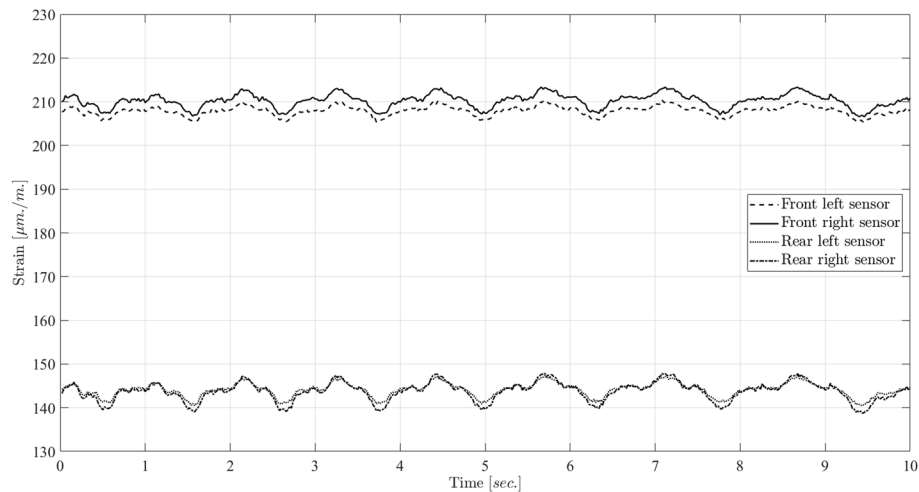

Fig. 14 The experimental static testing of the chassis for the first load case

Table 3 The numerical results of the chassis for the two load cases

	First load case		Second load case	
	Front support	**Rear support**	**Front support**	**Rear support**
Normal load	215 kg.	145 kg.	130 kg.	85 kg.
Distributed load	$W_C = \frac{215*9.81}{610}$ $= 3.4576 \, N/mm$	$W_D = \frac{145*9.81}{610}$ $= 2.3319 \, N/mm$	$W_C = \frac{130*9.81}{610}$ $= 2.0907 \, N/mm$	$W_D = \frac{85*9.81}{610}$ $= 1.367 \, N/mm$
Max. combined stress	37.94 Mpa		22.82 Mpa	
Max. strain	192 μm/m		115.4 μm/m	
Max. deformation	2.1 mm		1.26 mm	

Fig. 15 The strain gauge readings for the first load case

were acquired using an EDX-10A data acquisition system with 16 active channels. It was equipped to measure the real generated strain on the equivalent chassis using only four channels at 50 KHz sampling frequency over a 10-s duration. Then, the average value of the measured strain was conducted for validation and verification of the FE results.
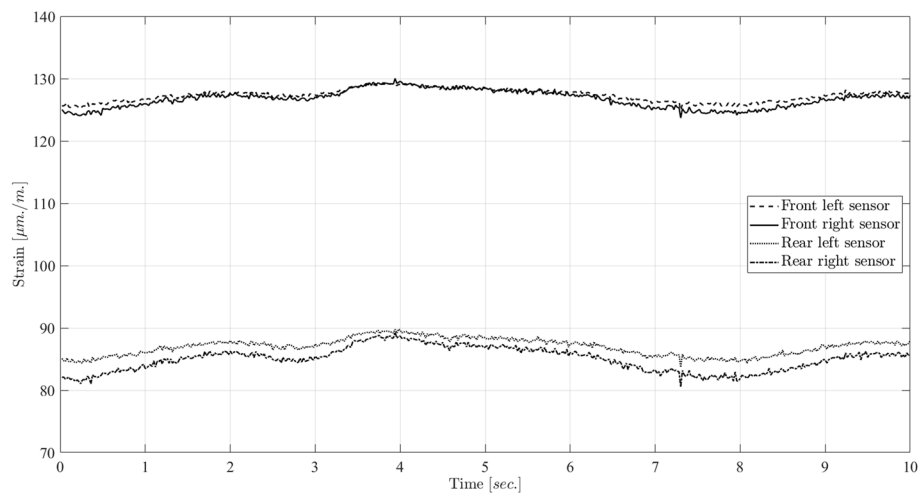
Results and discussion

Both the distributed loads acting on the supporting beams, maximum combined stress, maximum generated strains, and maximum deformation of the equivalent chassis were numerically calculated due to the vertical loading conditions for each load case, as illustrated in Table 3. For the first load case, vertically distributed loads of 3.4576 N/mm and 2.3319 N/mm were subjected to the front and rear support, respectively. Then, the maximum deformation of the chassis was 2.1 mm, with a maximum combined stress of 37.94 MPa, and a maximum strain of 192 μm/m. The strain gauge readings for the first load case are shown in Fig. 15. Also, a comparison between the experimental measurements and the numerical results for the first load case is illustrated in Table 4.

For the second load case, vertically distributed loads of 2.0907 N/mm and 1.367 N/mm were subjected to the front and rear support, respectively. Then, The maximum deformation of the chassis was 1.26 mm, with a maximum combined stress of 22.82 MPa, and a maximum strain of 115.4 μm/m. The strain gauge readings for the second load case

Table 4 A comparison between the FE results and the experimental results for the first load case

	Front left	Front right	Rear left	Rear right
Average strain from experimental test	207.91 μm./m.	210.24 μm./m.	144.11 μm./m.	143.72 μm./m.
Average strain from the FEA.	191.8 μm./m.	191.9 μm./m.	159.4 μm./m.	159.4 μm./m.
Error percentage	7.75%	8.72%	9.59 %	9.84%

Fig. 16 The strain gauge readings for the second load case

Table 5 A comparison between the FE results and the experimental results for the second load case

	Front left	Front right	Rear left	Rear right
Average strain from experimental test	127.32 μm./m.	126.75 μm./m.	86.98 μm./m.	85 μm./m.
Average strain from the FEA.	115.4 μm./m.	115.1 μm./m.	94.5 μm./m.	94.7 μm./m.
Error percentage	9.37%	9.19%	7.96%	10.24%

are shown in Fig. 16. A comparison between the experimental measurements and the numerical results for the second load case is illustrated in Table 5.

It was found that the error percentage between the experimental measurements and the FE results was from 7.75 to 9.84% for the first load case and from 7.96 to 10.24% for the second load case. The differences between the actual measurements and the numerical results may be due to the small differences in material properties, measurement deviations, chassis and test rig leveling errors, possible defects in welding, manufacturing, and assembly errors.

The effectiveness and feasibility of this study are to conduct the design optimization for a small-scale equivalent chassis of a low-bed semi-trailer. Also, it adopted a validation of the numerical analysis with the experimental test results for that small-scale chassis of the semi-trailer and the availability of performing the numerical analysis for the equivalent chassis to estimate the behaviors of the original semi-trailer. Besides, the possibility of using the numerical simulation of the original chassis for evaluating the structural responses under various loading conditions such as torsion, emergency braking, sudden acceleration, and high-speed cornering. This methodology

not only enhances the design effectiveness by minimizing the computational time but also reduces the required total expenses before starting mass production of the semi-trailer.

Conclusions

In this study, the focus was on designing and testing a small-scale prototype of a low-bed semi-trailer chassis to improve its weight, strength, reliability, and market competitiveness. The design process involved using finite element analysis (FEA) to optimize the chassis and reduce manufacturing costs. The optimized small-scale prototype was then manufactured and assembled by welding. Finally, two load cases were applied to the chassis to verify the FEA results with experimental measurements. The results showed an error percentage of 7.75 to 10.24% between the numerical analysis and the experimental results. These differences could be attributed to the small variations in material properties, weld properties, measurement deviations, possible weld defects, and manufacturing and assembling errors. The study highlights the importance of testing and verifying prototypes in the automotive industry to ensure that the final product meets desired standards.

Abbreviations

WHO	World health organization
FE	Finite element
FEA	Finite element analysis
CAD	Computer aided design
ISO	International organization for standardization
UPM	United paper mills
$I1_W, I1_H, I1_T$	Width, height, thickness of the first I cross-section respectively
$I2_H$	Height of the second I cross-section
$I3_W$	Width of the third I cross-section
$Box1_W, Box2_W$	Width of the first, the second box cross-section respectively
$Box1_T, Box2_T$	Thickness of the first, the second box cross-section respectively
ASO	Adaptive single-objective optimization
RSO	Response surface optimization
$\mathbf{x}$	Vector containing the design variables
$f(\mathbf{x})$	Total mass function
M	Total mass of the semi-trailer
$g(\mathbf{x})$	Objective function
e	Corresponding element number
n	Total number of elements
$\rho_e, A_e(\mathbf{x}), L_e(\mathbf{x})$	Corresponding element density, cross-section area, and length respectively
σ_e^B	Maximum combined stress
$\mathbf{x}_u, \mathbf{x}_l$	Upper, lower value of the design parameter respectively
MIG	Metal inert gas welding

Declarations

Ethics approval and consent to participate
Not applicable.

Consent for publication
Not applicable.

Competing interests
The authors declare that they have no competing interests.

References

1. World Health Organization. Global Status Report on Road Safety 2018 (Report No. ISBN 978-92-4-156568-4). Geneva: World Health Organization.
2. Sayed I, Abdelgawad H, Said D (2022) Studying driving behavior and risk perception: a road safety perspective in Egypt. J Eng App Sci. 69:22. https://doi.org/10.1186/s44147-021-00059-z
3. Sunday B, Bori I, Abdulkarim N, Nicholas AM (2021) Stability analysis of a semi-trailer articulated vehicle: a review. I J Aut Sci Tech. 5:131–140. https://doi.org/10.30939/ijastech.855733
4. Grislis A (2010) Longer combination vehicles and road safety. Tran. 25:336–343. https://doi.org/10.3846/transport.2010.41
5. Du X, Wang G (2022) Analysis of operating safety of tractor-trailer under crosswind in cold mountainous areas. App Sci. 12:12755. https://doi.org/10.3390/app122412755
6. Liimatainen H, Pöllänen M, Nykänen L (2020) Impacts of increasing maximum truck weight–case Finland. Euro Tran Res Rev. 12:1–12. https://doi.org/10.1186/s12544-020-00403-z
7. Thang TDV, Hoan NT, Hoang NM (2021) A research on reducing the weight of semi-trailer frame manufactured in Vietnam. J Sci Tech. 31:84–91. https://doi.org/10.51316/jst.150.ssad.2021.31.1.11
8. Koszalka G, Niewczas A, Golec M, Kaczor M, Taratuta L, Glowacz L (2013) A modular low-bed semi-trailer for transportation of machines and other heavy and big loads. J KONES Pow Tran. 20:237–244
9. Gauchia A, Diaz V, Boada MJL, Boada BL (2010) Torsional stiffness and weight optimization of a real bus structure. I J Aut Tech. 11:41–47. https://doi.org/10.1007/s12239−010−0006−4
10. Jang GW, Yoon MS, Park JH (2010) Lightweight flatbed trailer design by using topology and thickness optimization. Struc Multidisc Opt. 41:295–307. https://doi.org/10.1007/s00158-009-0409-x
11. Panganiban HP, Kim WC, Chung TJ, Jang GW (2016) Optimization of flatbed trailer frame using the ground beam structure approach. J Mech Sci Tech. 30:2083–2091. https://doi.org/10.1007/s12206-016-0415-z
12. Abd-Elhay AR, Murtada WA, Yosof MI (2022) A high accuracy modeling scheme for dynamic systems: spacecraft reaction wheel model. J Eng App Sci. 69:1–22. https://doi.org/10.1186/s44147-021-00056-2
13. Chen Y, Liu X, Yi H, He C, Xiao G, Tan J, Wu H, Su A (2022) Parameter optimization of rubber cylinder of expansion liner hanger based on numerical simulation. J Eng App Sci. 69:1–18. https://doi.org/10.1186/s44147-022-00086-4
14. Geneid AA, Atia MRA, Badawy A (2022) Multi-objective optimization of vertical-axis wind turbine's blade structure using genetic algorithm. J Eng App Sci. 69:90. https://doi.org/10.1186/s44147-022-00150-z
15. Swelem S, Fahmy A, Ellafy H (2022) Optimization of cold-formed lipped C-section under bending using prediction equations as objective functions. J Eng App Sci. 69:1–13. https://doi.org/10.1186/s44147-022-00106-3
16. Malon H, Tello L, Martin C (2011) Analysis and optimization of an innovative fatigue tests profile for three axle semi-trailers. AIP Conference Proceedings American Institute of Physics
17. Baadkar CC (2010) Semi-trailer structural failure analysis using finite element method. Dissertation, University of Canterbury.
18. Napierala R (2019) Numerical-experimental static analysis of the effort of the crossbar-longeron in the semi-trailer frame. AIP Conference Proceedings Publishing LLC
19. Deulgaonkar VR, Matani AG (2014) Development and validation of chassis mounted platform design for heavy vehicles. I J Veh Struct Sys. 6:51. https://doi.org/10.4273/ijvss.6.3.02
20. Akhtar MJ (2017) Development of guidelines for the selection of structural profiles to achieve optimized flooring structure. Dissertation, Aalto University.
21 Ibrahim AM, Ali AM, Kamel H (2022) Design and optimization of a missile transporter semi-trailer structure. J Phys Conf Ser 2299(1):012002
22. Thakur A, Aregawi GE (2019) Effect of heat treatment on mechanical properties and microstructure of ST 37–2 rear trailing arm. I J Curr Eng Tech. 9:80–91
23. ANSYS Help System (2020) ANSYS Inc (Accessed 1 June 2020)
24. Jang BS, Ko DE, Suh YS, Yang YS (2009) Adaptive approximation in multi-objective optimization for full stochastic fatigue design problem. Mar Struct. 22:610–632. https://doi.org/10.1016/j.marstruc.2008.11.001
25. Xiangjie J, Cai Z, Chong W (2020) Response surface optimization of machine tool columan based on ANSYS workbench. Acad J Man Eng 18:2
26. Keulen FV, Haftka RT, Kim NH (2005) Review of options for structural design sensitivity analysis. Part 1: Linear systems. Comput. Methods Appl. Mech. Engrg. 194:3213–3243. https://doi.org/10.1016/j.cma.2005.02.002

Publisher's Note

Springer Nature remains neutral with regard to jurisdictional claims in published maps and institutional affiliations.